

# NEU1 and NEU3 enzymes alter CD22 organization on B cells

Hanh-Thuc Ton Tran,<sup>1</sup> Caishun Li,<sup>1</sup> Radhika Chakraborty,<sup>1</sup> and Christopher W. Cairo<sup>1,\*</sup>

<sup>1</sup>Department of Chemistry, University of Alberta, Edmonton, Alberta, Canada

**ABSTRACT** The B cell membrane expresses sialic-acid-binding immunoglobulin-like lectins, also called Siglecs, that are important for modulating immune response. Siglecs have interactions with sialoglycoproteins found on the same membrane (*cis*-ligands) that result in homotypic and heterotypic receptor clusters. The regulation and organization of these clusters, and their effect on cell activation, is not clearly understood. We investigated the role of human neuraminidase enzymes NEU1 and NEU3 on the clustering of CD22 on B cells using confocal microscopy. We observed that native NEU1 and NEU3 activity influence the cluster size of CD22. Using single-particle tracking, we observed that NEU3 activity increased the lateral mobility of CD22, which was in contrast to the effect of exogenous bacterial NEU enzymes. Moreover, we show that native NEU1 and NEU3 activity influenced cellular Ca<sup>2+</sup> levels, supporting a role for these enzymes in regulating B cell activation. Our results establish a role for native NEU activity in modulating CD22 organization and function on B cells.

**WHY IT MATTERS** Glycosylation of membrane receptors and glycoproteins is an important factor in cell signaling. The most terminal residue of many glycans is sialic acid (N-acetylneuraminic acid), which is installed by sialyltransferases and removed by sialidase (also called neuraminidase) enzymes. One system known to be regulated by membrane sialic acids is CD22, a receptor that binds to *cis*- and *trans*-ligands containing sialic acids. In this study, we investigated whether CD22 receptor organization was affected by the activity of native neuraminidase enzymes. We also compare the effects of different neuraminidases from bacterial sources and the effect of chemical inhibitors of the enzymes. Our results suggest that native neuraminidase enzymes can modulate CD22 and its signaling.

## INTRODUCTION

B cell receptors (BCRs) are responsible for antigen recognition leading to B cell activation and proliferation in immune response. Regulation of B cell activation involves co-receptors that fine-tune BCR signaling. One widely studied negative regulator of BCR is CD22 (Siglec-2), a member of the sialic-acid-binding immunoglobulin-like lectin (Siglec) family (1). The structure and organization of CD22 on the cell membrane plays a crucial role in its activity. CD22 is a transmembrane protein containing seven immunoglobulin (Ig) domains that adopts a rod-like structure; the N-terminal Ig domain specifically recognizes terminal  $\alpha$ 2,6-sialic acids (2). The cytoplasmic portion of CD22 contains immunoreceptor tyrosine inhibitory motifs that dampen cellular response (3). CD22's lectin domain

can interact with sialosides from *cis*- or *trans*-ligands; however, the high density of *cis* sialosides on the membrane results in the formation of hetero- and homotypic clusters of CD22. The N-link glycans of CD22 allow for homotypic interactions (4,5), while heterotypic *cis*-binding partners, including CD45 (6,7), are known. Although CD22's ligand binding is somewhat weak (8), high-affinity *trans*-ligands can overcome *cis*-interactions despite their prevalence (9,10). High-affinity multivalent displays of CD22 ligands, including liposomes (11,12), polymers (4,10,13), and synthetic scaffolds (14), have been proposed as modulators of B cell activation.

The complexity of CD22 interactions and organization on the B cell membrane remains an active area of investigation. Previous studies have observed nano-clusters of CD22, with a minor role for the actin cytoskeleton in lateral mobility (15). Despite the large number of sialylated glycoproteins on the membrane, only a limited number of these have been identified as *in situ* CD22 ligands (5). This observation may

Submitted March 25, 2022, and accepted for publication July 19, 2022.

\*Correspondence: [ccairo@ualberta.ca](mailto:ccairo@ualberta.ca)

Editor: Erdinc Sezgin.

<https://doi.org/10.1016/j.bpr.2022.100064>

© 2022 The Authors.

This is an open access article under the CC BY-NC-ND license (<http://creativecommons.org/licenses/by-nc-nd/4.0/>).



indicate a role for membrane microdomains in enforcing specific interactions, as CD45 and IgM have close associations with lipid rafts (16–19). A common strategy for investigating the role of CD22-sialoside interactions is to use sialic-acid-cleaving enzymes: neuraminidases (NEUs, also called sialidases) (20). Recombinant NEUs from bacteria have been used for this purpose as research tools. NEU from *Clostridium perfringens* (NanI) has substrate preference for  $\alpha$ 2,3-glycoproteins, while the sialidase of *Arthrobacter ureafaciens* (siaAU) has a broader range of substrate specificity, cleaving  $\alpha$ 2,3-,  $\alpha$ 2,6-, or  $\alpha$ 2,8-linked gangliosides or glycoproteins. Exogenous NEU reagents have helped establish the importance of CD22-sialoside interactions; however, there has been very little work to investigate the role of native NEU enzymes on this system. There are four human NEU (hNEU) isoenzymes, NEU1, NEU2, NEU3, and NEU4, and they have important cellular functions and roles in health and disease (21), including atherosclerosis (22), malignancy (23–25), and neurodegenerative diseases (26–29). Together with glycosyl transferase enzymes, NEUs regulate sialic-acid content in cells (20). Thus, native NEU activity could act as a regulator of CD22 organization, B cell activation, and immune response.

Here, we investigated the influence of the cytoskeleton and native NEU activity on the membrane organization and dynamics of CD22. By utilizing confocal microscopy and single-particle tracking, we found that clustering and diffusion of these receptors are dependent on both cytoskeletal structure and changes in glycosylation of B cells. We confirmed our findings by performing knockdown of hNEU expression in model B cells. Finally, we confirmed that native hNEU activity affects B cell calcium levels. We conclude that organization and diffusion of CD22 receptors is dependent on an intact cytoskeleton and the homeostasis of native sialoside ligands.

## MATERIALS AND METHODS

### Confocal microscopy

Cells were grown in R10 media and kept in a humidified incubator at 37 °C and 5% CO<sub>2</sub>. For confocal microscopy experiments, Raji cells ( $1 \times 10^6$ ) were counted, centrifuged, and re-suspended in Hanks' balanced salt solution (HBSS). The cells were washed and treated with NanI (*Clostridium perfringens*), siaAU (*Arthrobacter ureafaciens*), or NEU3 in HBSS or cytochalasin D (CytoD) or latrunculin A (LatA) in HBSS with 0.005% dimethyl sulfoxide at 37 °C for 30 min then fixed using 1% paraformaldehyde on ice for 30 min. Samples were treated with 1  $\mu$ L/mL mouse anti-human IgM (clone IM260, Abcam, Cambridge, UK, cat# ab200541) or mouse anti-human CD22 (clone HIB22, BD Pharmingen, San Diego, CA, USA, cat# 555423) at 4 °C overnight and stained with goat anti-mouse IgG (polyclonal, Sigma-Aldrich, Burlington, MA, USA, cat# M8642) conjugated with Alexa Fluor 647 (AF647) at room temperature for 1 h. The loading of the fluoro-

phores was approximately 2 dyes/protein. After washing, samples were transferred to 24-well plates (Corning, Corning, NY, USA) with circular cover glass slides pre-treated with poly-L-lysine, spun at  $300 \times g$  for 15 min and washed, and glass slides were mounted onto microscopy slides with Slowfade Antifade (Thermo Fisher Scientific, Waltham, MA, USA, cat# S2828) and sealed using Cytoseal 60. Samples were imaged on a laser scanning confocal microscope (Olympus IX81 with 60 $\times$  objectives). Twenty cells from each condition were chosen for analysis based on transmitted and fluorescence images, and each cluster was analyzed using the particle analysis function (size, 0–infinity  $\mu$ m<sup>2</sup>; circularity, 0.00–1.00) on ImageJ without segmentation. The image thresholding was kept consistent between runs by adjusting to a value that did not identify clusters in the negative controls. Acquisition settings were kept identical between runs (laser intensity, 20%; PMT, 500; gain, 3 $\times$ ; offset, 5%), and negative controls were run in each experiment to confirm that levels were properly set. The data were plotted using the beanplot plugin in R, and statistics were done using GraphPad Prism. Three runs were performed and analyzed, and one representative run is shown for each condition. We confirmed that clusters of CD22 were stable after fixation.

### Single-particle tracking

Raji cells were grown in R10 media as previously described (14). For each condition, cells ( $1 \times 10^6$ ) were counted and washed with HBSS buffer three times. The cells were then re-suspended in HBSS and treated with NanI (10 mU/mL), siaAU (5 or 10 mU/mL), or NEU3 (10 mU/mL). For CytoD and LatA, the cells were re-suspended in 0.005% dimethyl sulfoxide, and the compounds were added to a final concentration of 0–10 (0–20  $\mu$ M) or 0–0.5  $\mu$ g/mL (0–1.2  $\mu$ M), respectively. For all conditions, the cells were incubated for 30 min at 37 °C and 5% CO<sub>2</sub>. After incubation, the cells were centrifuged and washed three times with HBSS buffer at  $200 \times g$  for 15 min, re-suspended in HBSS, and labeled with anti-CD22 conjugated with AF647 (1 h at room temperature). After labeling, the cells were washed three times in buffer then transferred to 24-well plates with circular glass covers pre-treated with poly-L-lysine. The plate was then spun at  $300 \times g$  for 15 min, and the cover glass was mounted to microscope slides with buffer and sealed with Cytoseal 60. To record the trajectories, total internal fluorescence microscopy was performed on Nikon Ti microscope. The angle of incidence was set at  $\sim$ 1,100, and videos were taken at 10 frames per s for 10 s (30). All videos were taken within 1 h of slide preparation. Trajectories were analyzed using UTrack software in MATLAB, and the coefficient of diffusion was calculated using MATLAB.(30).

### Transfection of Raji cells

Raji cells were grown as described and passaged 24 h prior to transfection (14). Cells ( $24 \times 10^6$ ) were washed and re-suspended into 750  $\mu$ L electroporation buffer (PBS with no Ca<sup>2+</sup> or Mg<sup>2+</sup>). For each knockdown condition, 15  $\mu$ L from the 20  $\mu$ M stock small interfering RNA (siRNA) solution was added, while 15  $\mu$ L siRNA buffer was added for the no-treatment control. Cells were mixed by pipet and transferred to a 2 mm electroporation cuvette. Cell samples were left on ice for 20 min, and electric shock was applied using a Bio-Rad electroporator (0.6 kV, 50  $\mu$ F, and 350  $\Omega$ ). The cuvettes were then immediately transferred and left on ice for 30 min. Transfected cells were transferred to T25 cell culture flasks, and pre-warmed R10 growth medium was added so the final volume for each condition was 6 mL. Cells were kept in a humidified incubator at 37 °C with 5% CO<sub>2</sub> for 24 h.

## Ca<sup>2+</sup> activity assay of Raji cells

For each condition, Raji cells were counted and re-suspended to a final concentration of  $1 \times 10^6$  cells/mL. Cells were then treated with NEU at a final concentration of 10 mU/mL or with 100 nM NEU inhibitors. For treatments of enzyme with inhibitors, these were incubated together for 30 min before addition to cells. The cells were treated with indicated conditions for 1 h at 37 °C with 5% CO<sub>2</sub>. For transfected cells, cells were transfected and grown 24 h prior to Ca<sup>2+</sup> experiments. Cells were washed three times with PBS and re-suspended at  $5 \times 10^6$ /mL in loading buffer (RPMI-1640 supplemented with 1% FBS, 10 mM HEPES, 1 mM MgCl<sub>2</sub>, 1 mM EGTA, and 5% penicillin-streptomycin) and treated with 1.5 μM Indo-1 dye in a 37°C water bath for 30 min while protected from light. After loading, the cells were washed with loading buffer three times, then re-suspended in running buffer (HBSS supplemented with 1% FBS, 1 mM MgCl<sub>2</sub>, and 1 mM CaCl<sub>2</sub>), after which they were stored on ice. Using a Fortessa X10 FACS machine, a plot of violet (379 nm) versus blue (450 nm) was created, and voltages were adjusted so that a maximum of 5% of unstimulated cells lie within the violet gate. To measure the amount of Ca<sup>2+</sup> flow into the cells, 500 μL of previously suspended cells from each condition were transferred to fluorescence-activated cell sorting tubes incubated in 37°C water bath for 2 min before running the samples. Ten seconds after the acquisition was initiated to establish the background, the tube was quickly removed, and either PBS (unstimulated condition) or anti-IgM (stimulated condition) was added and vortexed before placing the tube back. The total acquisition time was 3 min for each tube, and the number of cells analyzed ranged from 150,000 to 400,000 cells. From these data, the percentage of cells emitting violet light from each condition was normalized to that of control unstimulated cells, and statistics were performed with GraphPad Prism (31).

## Western blot of Raji cells

Transfected cells were centrifuged, and supernatant was discarded. The cells were lysed using 100 μL HEPA buffer with protease inhibitor on ice for 1 h. The lysate was sonicated and centrifuged at  $12,000 \times g$  for 20 min. Supernatant was collected, and the amount of protein was determined using BCA assay. For each condition, 10 μg protein was mixed with the same volume of 2X gel running buffer with 5% dithiothreitol, followed by 5 min incubation at 95 °C. After heating the samples, they were then transferred to an 11% acrylamide gel, and SDS-PAGE was run at 110 V for 70 min. After the gel was completed, it was washed with water and transferred to a nitrocellulose membrane in 1X blotting buffer at 20 V for 2.5 h. Once the transfer was completed, the transfer of proteins was confirmed by soaking the membrane in Ponceau S buffer for 5 min, washing the membrane with water, and checking for presence of bands on the membrane. The membrane was blocked in blocking buffer (5% non-fat milk in 1X TBST) on an orbital shaker overnight at 4 °C. The membrane was then washed three times with TBST for 5 min each time. The membrane was stained using primary antibody in TBST with 1:1,000 dilution for 1 h at room temperature. The membrane was washed 5 times with TBST then stained using secondary antibody conjugated with horse radish peroxidase with 1:10,000 dilution in TBST for 1 h at room temperature. The membrane was washed and developed using enhanced chemiluminescence substrate for Western blotting and visualized. The percentage of knockdown was determined by analyzing the intensity of each band using ImageJ. The samples were normalized to the control, and a Student's *t*-test was implemented for analysis.

## Lectin blots

CD22 proteins were purified from Raji cells using murine hybridoma cells expressing anti-CD22 antibodies ( $\alpha$ -CD22:4213 (10F4.4.1)). The purified sample was validated by SDS-PAGE, and the protein concentration was determined using a BCA assay. From the stock solution, 4.4 μg protein was diluted to a final volume of 200 μL and enzyme concentration of 10 mU/mL, then the samples were incubated at 37 °C for 3 hours. After treatment of the proteins with enzyme, each sample was mixed with the same volume of 2X PAGE sample buffer with SDS, then 40 μL from each sample was subjected to SDS-PAGE with 10% acrylamide at 110 V for 70 min. For each of the samples, three lanes were loaded together with control samples. Gels were then taken out, washed three times with water, and transferred to a nitrocellulose membrane. The presence of proteins on the membrane was confirmed using Ponceau S, then they were cut so that a control and an enzyme-treated lane were retained. The membranes were washed with TBST and blocked with blocking buffer (5% non-fat milk in TBST) at 4 °C overnight. Membranes were washed three times with TBST, then treated with 1 μg/mL biotinylated lectins (PNA, SNA, MAL) at room temperature for 1 h. The treated membranes were washed 5 times with TBST and treated with streptavidin-HRP for 1 h at 1:10,000 dilution, followed by washing the membranes with TBST. The bands were detected using enhanced chemiluminescence substrate for Western blotting under a visualizer. The analysis of the bands was conducted using ImageJ.

## RESULTS

### Cytoskeletal interactions of BCR

To study the effect of cytoskeletal contacts on BCR, we used Raji cells treated with cytoskeletal disruptors CytoD and LatA as a model B cell system. Microclusters of BCR are known to form when B cells are stimulated due to the association of the constant region C<sub>μ</sub>4, followed by phosphorylation that induces cellular response (32). Several studies have observed cytoskeletal interactions with BCR, and the effect of cytoskeletal disruption was increased BCR cluster size and cell activation (33,34). Cells were treated, fixed, and imaged by confocal microscopy, allowing quantitation of cluster size (Fig. 1) (14). CytoD and LatA were used to disrupt the cytoskeleton (35–38). We observed a significant increase in clustering of BCR upon treatment with both inhibitors at all concentrations (15), and there was significantly increased clustering at lower concentrations compared with higher concentrations (2.5 versus 7.5 μg/mL;  $p < 0.05$ ) (39).

### Cytoskeletal interactions of CD22

We next examined the cytoskeletal interactions of CD22 in a B cell model. Analysis of CD22 clustering after treatment with cytoskeletal disruptors is shown in Fig. 2. We observed that CD22 cluster size increased significantly when cells were treated with CytoD. Interestingly, the cluster size was increased at intermediate concentrations (2.5–7.5 μg/mL); however, this effect

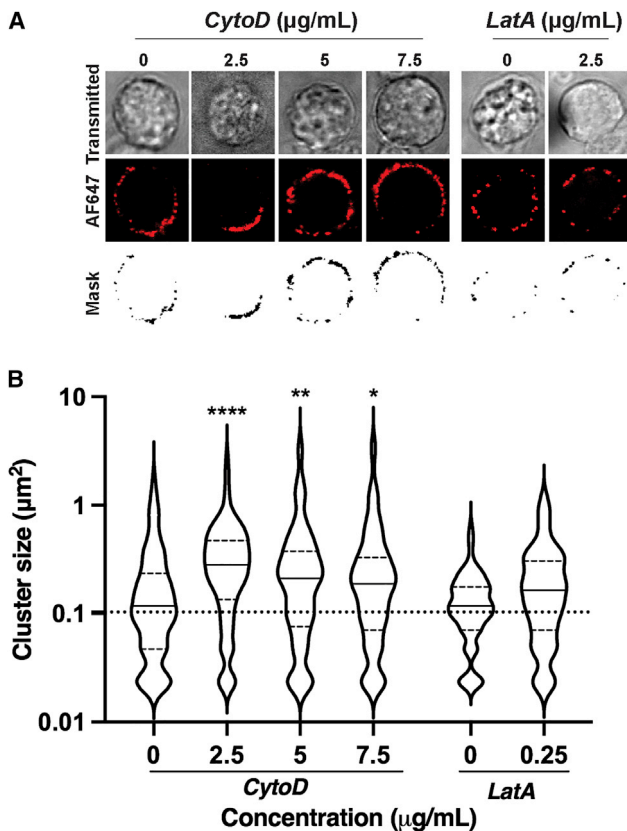


FIGURE 1 Cluster size of BCR after treatment with cytoskeletal disruptors. Raji cells were treated with cytochalasin D or latrunculin A at 37 °C for 30 min. (A) Cells were then fixed and stained with mouse anti-IgM and anti-mouse IgG-AF647 and imaged using confocal microscopy. (B) Data shown are average from 30 cells among 3 biological replicates, with an n of 100 to 200 clusters for each condition. Cells were analyzed using ImageJ and are shown as beanplots (14). Comparison analyses were done using a one-way ANOVA followed by Dunnett's *t*-test (\*\*\*\**p* < 0.0001; \*\**p* < 0.01; \**p* < 0.05).

was lost at higher concentrations (10 µg/mL). Similar trends have been observed in tight junctions and may be attributed to different populations of actin within the cell (39,40). Previous work has suggested that CytoD does not alter CD22 clustering or organization in the membrane; however, these studies were performed at high drug concentrations (10 µM; 5 µg/mL), and our results suggest that lower concentrations show greater effects in this system (15). Treatment of cells with LatA showed no effect on the cluster size of CD22 at the concentrations tested (0.050–0.500 µg/mL). One explanation for this difference is the disparate mechanisms of actin disruption used by these two inhibitors (38). Alternatively, the incubation time with LatA (30 min) may have been insufficient (41,42).

We next investigated if cytoskeletal interactions had a significant influence on the lateral mobility (diffusion) of CD22 in the membrane. We employed single-particle

tracking (SPT) using total internal fluorescence microscopy to measure changes in CD22 membrane diffusion (30). Raji cells were stained with minimal amounts of AF647-conjugated primary antibody to CD22. This sparse labeling allowed visualization of CD22 trajectories on live cells, which could be converted to rates of diffusion (Fig. 3) (43). This method allowed us to compare lateral diffusion of proteins in control and cytoskeleton-disrupted conditions. Treatment with CytoD at low concentrations (2.5 µg/mL) significantly decreased CD22 diffusion; however, at higher concentrations (10 µg/mL), this effect was lost. We note that at the highest concentration of CytoD, the distribution of trajectories shows an increase in mobile trajectories. Treatment with LatA (0.25 µg/mL) did not show a significant decrease in lateral mobility of CD22.

### NEU1 and NEU3 activity alter CD22 cluster size

Considering that the lectin activity of CD22 is dependent on sialylated *cis*-ligands, we next investigated if native hNEU enzymes could alter CD22 membrane organization. CD22 is found in homotypic clusters (5,44) and also has *cis* interactions with other sialylated proteins, including CD45 (45–47). We developed an siRNA knockdown protocol using electroporation for NEU1 and NEU3 enzymes (48), as lymphocytes are often difficult to transfect using lipid-based methods. The reduced expression of NEU1 and NEU3 was confirmed by Western blot of the transfected cells (Figs. 4 A, B, and S1). We found that B cells treated with siRNA for *Neu1* or *Neu3* had expression of the enzymes reduced by approximately half. Viability of the cells by hemocytometer after treatment showed no significant decrease for *Neu1* siRNA, while *Neu3* siRNA did show a decrease in viability (Fig. S2). We proceeded to determine if NEU1 and NEU3 knockdown (KD) cells showed evidence of changes to CD22 membrane organization. Analysis of clustering in these cells found a significant increase in CD22 cluster size in NEU1 KD cells, and some of these cells exhibited large clusters that could be described as polarization. In contrast, NEU3 KD cells had a significant decrease in cluster size, suggesting that these two isoenzymes play different roles in regulating CD22 organization (Fig. 4 C). This observation can be partly attributed to the different substrate specificities of the two enzymes. NEU1 is known to prefer glycoprotein substrates and NEU3 to prefer glycolipids (20,49). Thus, each isoenzyme could favor changes to glycolipid or glycoprotein sialosides. Additionally, the expression levels of these two enzymes may vary in lymphoid cells, with NEU1 generally being found at higher expression in many cell types (50,51).

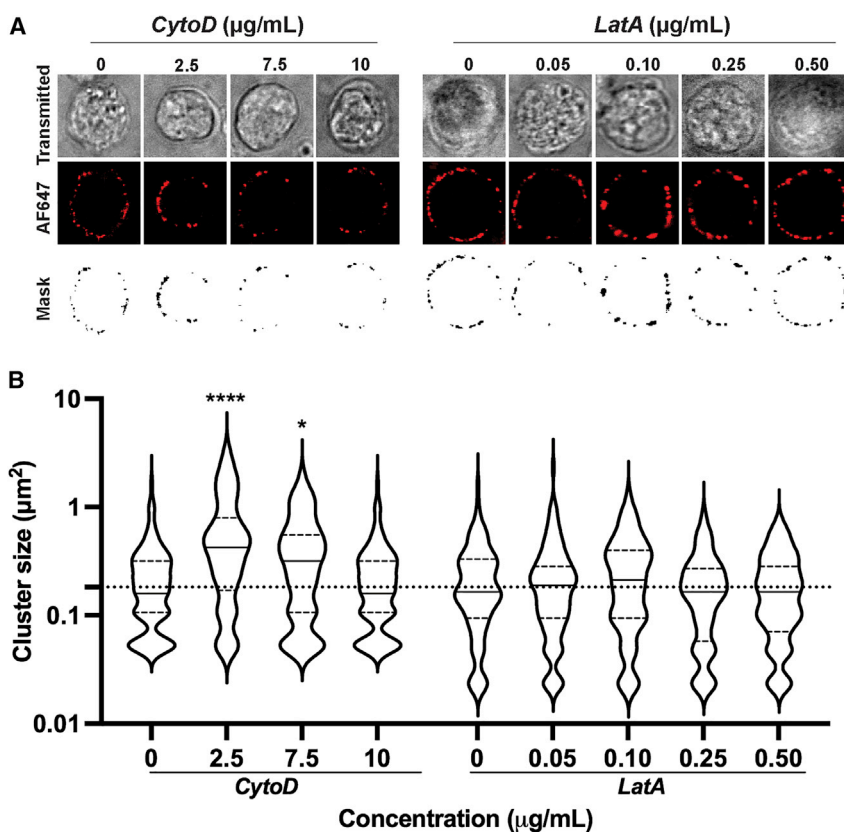


FIGURE 2 Cluster size of CD22 after treatment with cytoskeletal disruptors. Raji cells were treated with cytochalasin D or latrunculin A at 37 °C for 30 min. (A) Cells were then fixed and stained with mouse anti-CD22 and anti-mouse IgG-AF647 and imaged using confocal microscopy. (B) Data shown are average from 30 cells among 3 biological replicates. *n* values for conditions were 100 to 200 clusters. Cells were analyzed using ImageJ and are shown as beanplots (14). Comparison analyses were done using a one-way ANOVA followed by Dunnett's *t*-test (\*\*\*\**p* < 0.0001; \**p* < 0.05).

### Native NEU modulate B cell activation

The CD22 receptor acts as a negative regulator of B cell activation, and the organization and engagement of CD22 can alter B cell response (52). We investigated the role of NEU1 and NEU3 in B cell activation using a ratiometric calcium assay with Indo-1 dye by flow cytometry (31,53,54). We first asked if small-molecule inhibitors of NEU enzymes had a measurable effect on B cell activation (Fig. 5) (55). We used three different compounds: DANA, a pan-selective inhibitor of NEU enzymes; CG33300, a NEU1-selective inhibitor; and CG22600, a NEU3-selective inhibitor (56–58). When all conditions were normalized to the control group, we observed that treating B cells with DANA increased basal activation. Additionally, cells treated with DANA and anti-IgM showed a significant increase in activation relative to control. Although these observations are consistent with native NEU activity acting as a negative regulator of B cell activation, they did not indicate which enzymes were involved. The selective NEU1 inhibitor CG33300 showed similar effects to DANA—increased B cell activation relative to unstimulated and stimulated controls (Fig. 5 B). A selective NEU3 inhibitor, CG22600, showed similar activity—enhancing cell activation in basal and stimulated cells (Fig. 5 C). From these experiments, we concluded that native

hNEU enzymes, including NEU1 and NEU3, act as negative regulators of B cell activation. We sought to confirm the role of NEU1 and NEU3 on B cell activation using siRNA KD conditions. Transfected B cells were subjected to a Ca<sup>2+</sup> assay as described above after KD of NEU1 or NEU3 and compared with a scrambled control RNA control (Fig. 6). We found that both NEU1 and NEU3 KDs had increased basal Ca<sup>2+</sup> levels in cells, consistent with our inhibitor studies.

One possible explanation for changes to B cell activation after siRNA transfection is differences in CD22 expression after treatment. We tested for changes in CD22 expression using flow cytometry following siRNA treatments (Fig. 7). We found no significant change in CD22 expression levels between scrambled control RNA and NEU1 KD or NEU3 KD samples. We concluded that the changes we observed for CD22 clustering were not a result of large changes in expression levels.

### Exogenous NEU affect CD22 organization and B cell activation

A common strategy for probing the role of membrane sialosides in signaling is to treat cells with exogenous NEU enzymes. Typical examples include the sialidase from *Arthrobacter ureafaciens* (siaAU) and NanI from

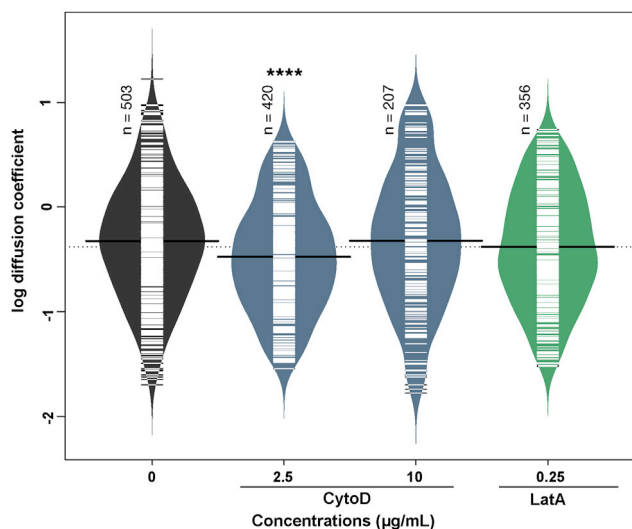


**FIGURE 3** Lateral mobility of CD22 after treatment with cytoskeletal disruptors. Raji cells were treated at 37 °C for 30 min. Lateral mobility was analyzed using single-particle tracking with total internal fluorescence microscopy videos recorded at 10 frames per s for 10 s (30). Diffusion coefficients are given as  $\log(D)$ , where  $D$  is in units of  $\times 10^{-10}$  [ $\text{cm}^2\text{s}^{-1}$ ] or  $\times 10^{-2}$  [ $\mu\text{m}^2\text{s}^{-1}$ ]. 150 cells among 3 biological replicates were analyzed, and values were compared with control using one-way ANOVA followed by Dunnett's test (\*\*\*\* $p < 0.0001$ ). Beanplots were generated using R software. Individual data points are represented by short white lines, a solid black line indicates the average for each condition, and the dotted line represents an average across all populations.

*Clostridium perfringens*. These enzymes have different specificities, with siaAU having broad activity to cleave  $\alpha$ 2,3- and  $\alpha$ 2,6-linkages (59,60), while the latter prefers  $\alpha$ 2,3-linked sialosides (61). It is worth noting that these enzymes have different substrate specificity from

hNEU isoenzymes and may not be good biochemical proxies for the native enzymes (20). We found that treatment of B cells with NanI and siaAU generally increased clustering of CD22 (Figs. S3 A and C) but not BCR (Fig. S4). We noted that the effect on CD22 cluster size was dependent on the activity of enzyme used—with high specific activity of siaAU (10 mU/mL) reversing significant increases seen at lower activity (5 mU/mL). Analysis of B cells treated with these enzymes by SPT found that CD22 lateral mobility was significantly reduced for NanI, but not siaAU, treatment (Fig. 8). This result is similar to observations with CytoD treatment, where increased clustering of CD22 was coincident with decreased lateral mobility.

We next investigated if exogenous hNEU3 enzyme had similar effects to the bacterial NEU enzymes on clustering and diffusion of CD22. When B cells were treated with NEU3 (10 mU/mL), clustering of CD22 significantly increased, consistent with the effect of the bacterial enzymes (Fig. S3B). Measurements of the lateral mobility of CD22 after NEU3 treatment showed an increase in diffusion (Fig. 8). We performed an analysis of B cell glycosphingolipids after exogenous NEU treatment using liquid chromatography-mass spectrometry (Fig. S5) (30), in which we observed no significant changes for any of the enzyme treatments. This may suggest that changes to glycosphingolipid composition are not the major factor in changes to CD22 organization or that these changes in composition are below the detection limit of our assay. An alternative explanation for changes to CD22 organization is that exogenous NEU enzymes modify CD22 glycosylation, thus altering homotypic clustering. Using purified CD22, we confirmed that

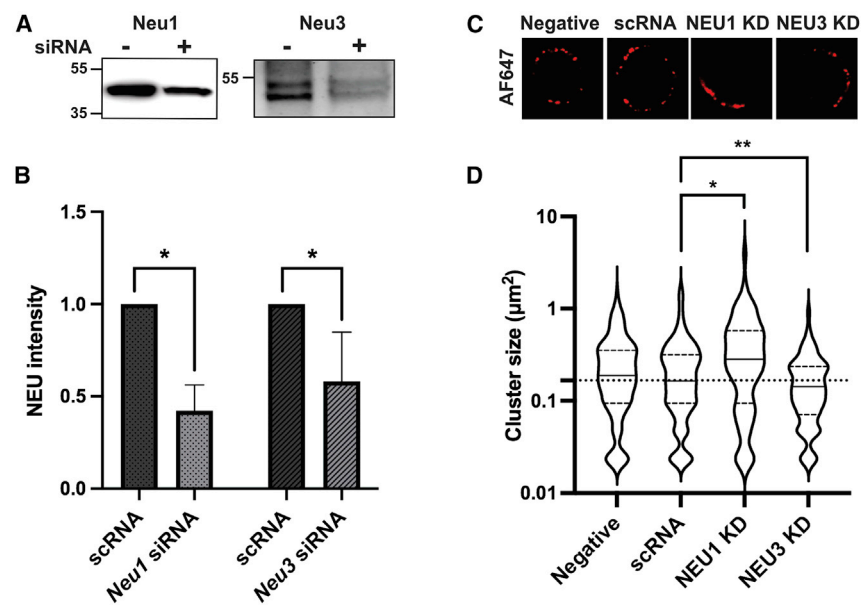


**FIGURE 4** CD22 cluster size is altered by NEU1 and NEU3 knockdown. Raji cells were transfected with siRNA targeting *Neu1* or *Neu3* using electroporation and grown for 24 h. (A) Western blots of transfected Raji cells. (B) Quantification of Western blots confirmed reduced expression of NEU1 and NEU3. (C and D) After transfection, Raji cells were fixed and stained with mouse anti-CD22 and anti-mouse IgG-AF647 and imaged using confocal microscopy (C) to determine the (D) cluster size of CD22. Data shown are average from 30 cells among 3 biological replicates.  $n$  values for each condition were between 100 and 200 clusters. Cells were analyzed using ImageJ and are shown as beanplots (14). Comparison analyses were done using one-way ANOVA followed by Dunnett's  $t$ -test (\*\* $p < 0.01$ ; \* $p < 0.05$ ).

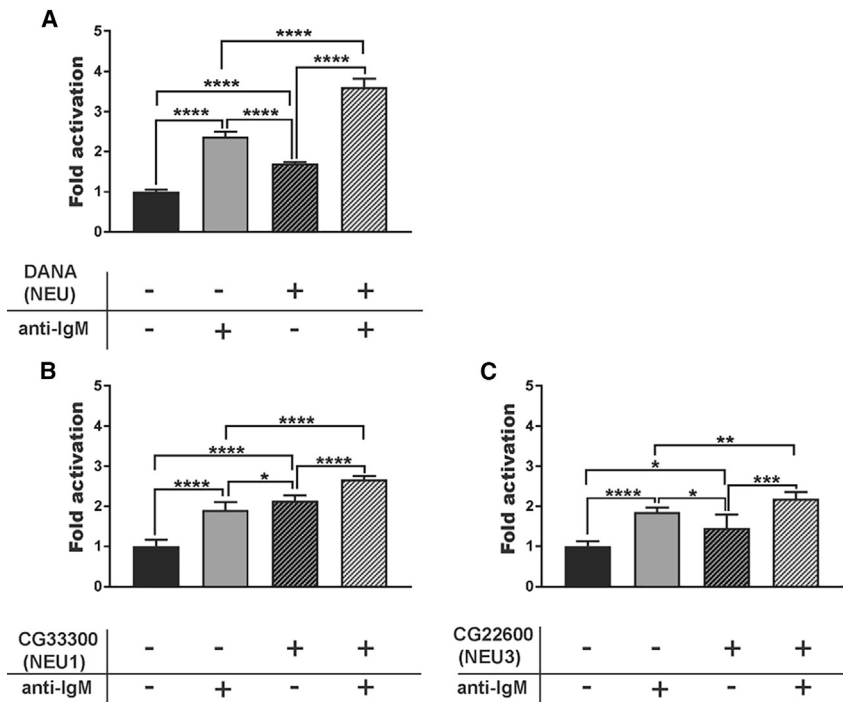


FIGURE 5 B cell response after treatment with NEU inhibitors. (A–C) Raji cells were incubated at 37 °C for 30 min with NEU inhibitors: (A) DANA (100  $\mu$ M), (B) CG33300, a NEU1 inhibitor (10  $\mu$ M), or (C) CG22600, a NEU3 inhibitor (10  $\mu$ M). Cells were either untreated (–, saline) or treated with inhibitor (+), followed by activation with anti-IgM. Activation of cells was monitored by observing  $Ca^{2+}$  levels by Indo-1 dye (31). For each treatment, 6 technical replicates from each of 3 biological replicates were performed. Responses were normalized to that of saline-treated and unstimulated control groups and compared by Student's *t*-test (\*\*\*\**p* < 0.001; \*\*\**p* < 0.005; \*\**p* < 0.01; \**p* < 0.05).

NanI and siaAU reduced SNA staining and increased PNA staining for CD22, consistent with desialylation of the receptor *in vitro* (Figs. S6 and S7).

During our studies, we encountered an issue that may complicate experiments that use exogenous bacterially-produced NEUs. Exogenous enzymes from bacterial sources may contain lipopolysaccharides (LPSs), and this contaminant may affect lymphocyte activation (62–64) or CD22 expression (65). We found that samples of siaAU and NanI from commercial sources

contained more than 1 endotoxin unit/mL (1 endotoxin unit = 0.1–0.2 ng), with final LPS concentrations in our experiments of 0.0001–0.01 ng/mL. We tested whether these amounts of LPS alone could affect CD22 clustering (Fig. S8). We observed a significant increase in CD22 clustering at 0.01 ng/mL of LPS in our assay, while higher concentrations attenuated this effect (0.1 ng/mL). Additionally, determinations of B cell activation using  $Ca^{2+}$  level assays after treatment with exogenous siaAU or NanI were ambiguous in our hands (Fig. S9). For example, siaAU at lower concentrations had similar effects to treatment with DANA (Fig. S9A versus Fig. 5 A) despite the fact that these treatments should have opposite effects on sialic-acid content on cells. Higher concentrations of siaAU attenuated this effect (Fig. S9 B), while NanI treatment showed no significant differences from control (Fig. S9 C).

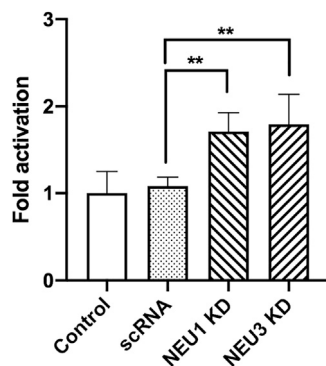


FIGURE 6 B cell calcium levels after NEU1 and NEU3 knockdown. Raji cells were transfected with siRNA targeting *Neu1*, *Neu3*, or a scrambled control using electroporation. Cells were grown for 24 h, and  $Ca^{2+}$  levels were monitored using Indo-1 dye (31). For each treatment, 2 technical replicates from each of 3 biological replicates were performed. Responses were normalized to that of saline-treated and unstimulated control groups and compared by Student's *t*-test (\*\**p* < 0.01).

## DISCUSSION

The data described here provide critical insight into the effects of native and exogenous NEU enzymes on CD22 organization on B cells. The organization of CD22 on the membrane is dependent on the lectin activity of the receptor and the availability of sialoglycoproteins in the milieu of the plasma membrane. We set out to understand if native NEU enzymes, which help regulate levels of sialylation of glycolipids and glycoproteins, could influence CD22 organization. Using

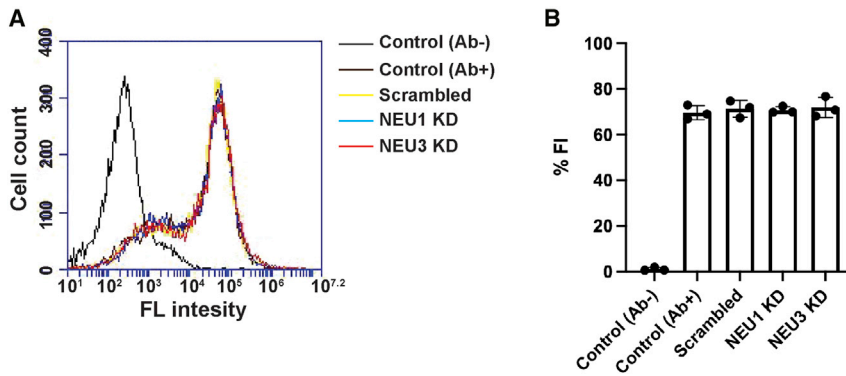


FIGURE 7 CD22 expression after NEU1 and NEU3 knockdown. Raji cells were transfected with siRNA targeting *Neu1*, *Neu3*, or a scrambled control using electroporation. Cells were allowed to grow for 24 h, collected, and stained using mouse anti-CD22 primary antibody and goat anti-IgG secondary antibody. (A and B) A histogram of the fluorescence channel is shown (A), and quantitation of these data found no changes in expression for the siRNA treatments (B).

confocal microscopy and SPT, we demonstrated that CD22 has interactions with the cytoskeleton, though we did not resolve the nature of this interaction. We found that native NEU1 and NEU3 activity influenced both the size of CD22 clusters and their mobility within the membrane. Based on our results, we conclude that increased NEU1 activity led to smaller CD22 clusters. In contrast, increased NEU3 activity (both native or exogenous) generated larger CD22 clusters, which had increased diffusion. Moreover, exogenous bacterial NEU activity generated larger CD22 clusters with decreased diffusion. These stark differences were likely the result of different substrate specificities for each enzyme. Importantly, we confirmed that LPS contamination in exogenous enzyme preparations influenced CD22 organization and could complicate at-

tempts to use these reagents to understand the role of CD22 interactions with *cis* sialoside ligands. Furthermore, we confirmed that native NEU activity influenced B cell response to BCR clustering using a  $\text{Ca}^{2+}$  assay. KD or chemical inhibition of both NEU1 and NEU3 enzymes resulted in increased basal activation of B cells, consistent with these enzymes acting as negative regulators of B cell stimulation. Our studies clearly support the involvement of the cytoskeleton and NEU enzymes in regulating CD22 organization and B cell activity. One limitation of our study is that we used only one cell line (Raji), which may not be representative of primary B cells. Raji cells may have differences in internalization rates of CD22 (66), glycosylation of CD45 (67), and expression of galectins (68) compared with primary B cells. Additionally, we used chemical fixation

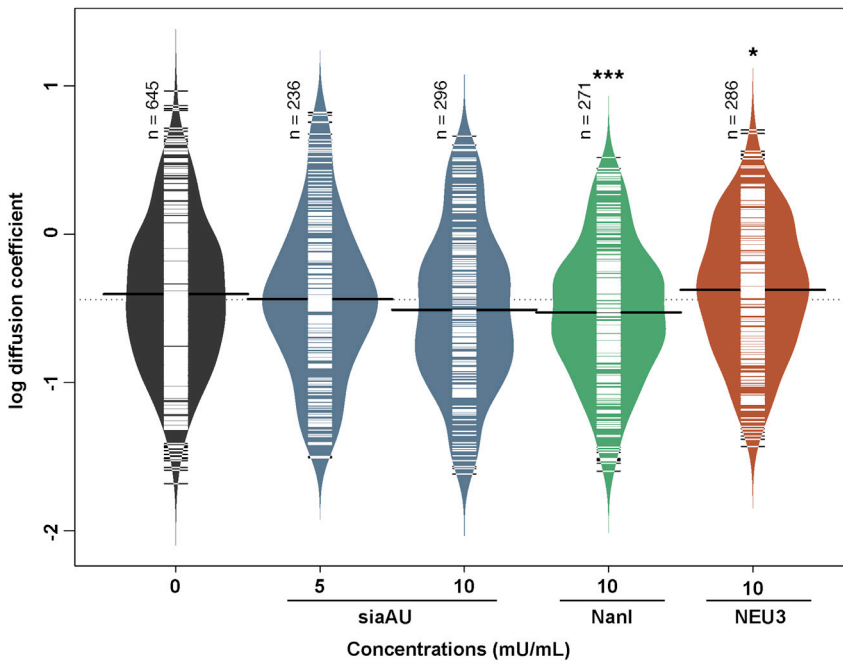


FIGURE 8 Lateral mobility of CD22 after treatment with NEU enzymes. Raji cells were treated at 37 °C for 30 min. Lateral mobility was analyzed using single-particle tracking with total internal fluorescence microscopy videos recorded at 10 frames per s for 10 s (30). Diffusion coefficients are given as  $\log(D)$ , where  $D$  is in units of  $\times 10^{-10} [\text{cm}^2\text{s}^{-1}]$  or  $\times 10^{-2} [\mu\text{m}^2\text{s}^{-1}]$ . Data shown are from 150 cells among 3 biological replicates. Data were analyzed and compared with control using a one-way ANOVA followed by Dunnett's test (\*\* $p < 0.005$ ; \* $p < 0.05$ ).

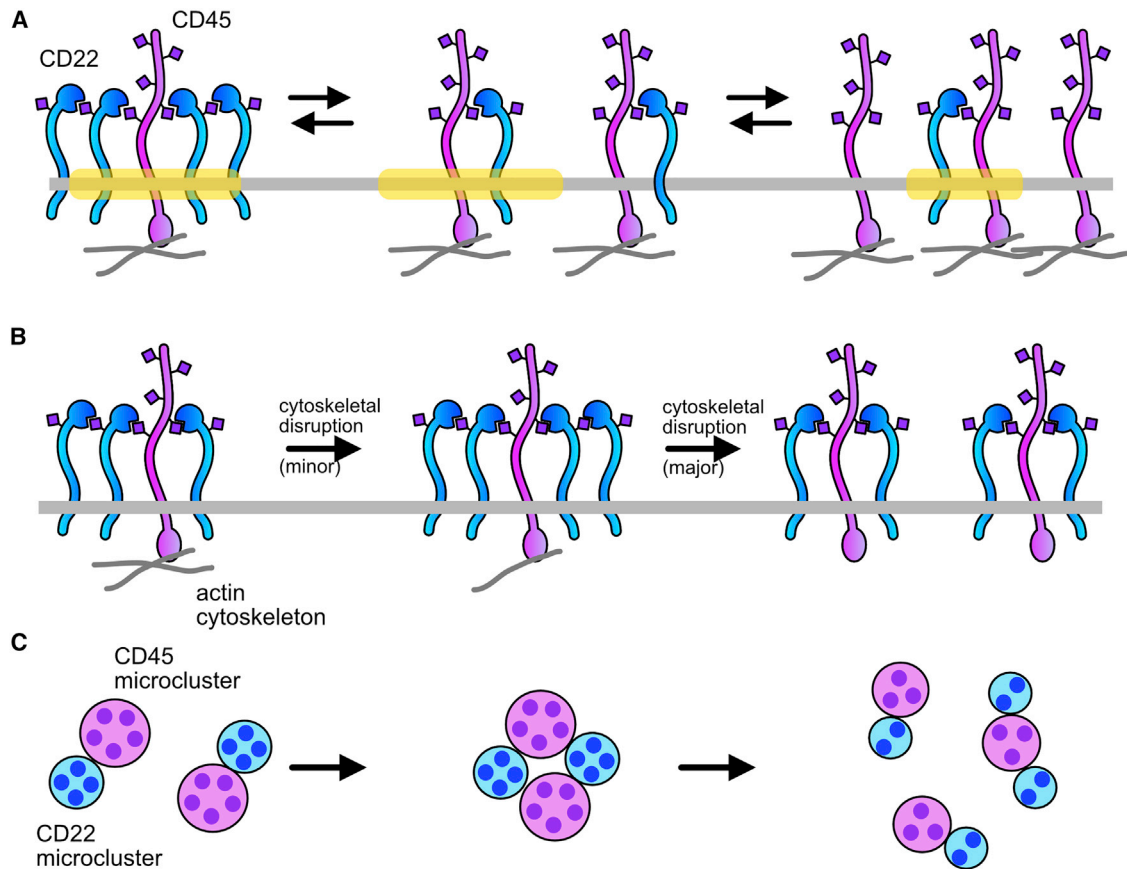


FIGURE 9 Model of changes in CD22 organization. (A) The size of the CD22 cluster formed is a result of interactions between CD22 and sialylated ligands, such as CD45, which can act as a bridge to homoclusters. A change in the stoichiometric ratio will shift the amount of complex (e.g., excess of the sialoside ligand or CD22). Increased NEU activity could reduce the total number of sialylated ligands available for CD22. (B) Cytoskeletal disruption allows microclusters of sialoglycoproteins to reorganize and act as a bridge to generate larger CD22 clusters. More extensive cytoskeletal disruption alters microclusters, leading to more diffuse clusters of both components. (C) A top-down representation of changes to cluster size due to cytoskeletal disruption.

of cells in our clustering studies, and some portion of receptors may remain mobile in these conditions.(69).

Lateral mobility of immune cell receptors is complex and can be influenced by a number of factors (70) such as the lateral size of the protein (71), cytoskeletal barriers (72–75), the presence of membrane microdomains (76), and crowding effects (77). Studies have proposed CD22 (15), CD45 (78), and BCR (79,80) are associated with membrane microdomains in lymphocytes (19,81). CD22 is not thought to have direct contacts to the cytoskeleton, though *cis*-ligands could provide indirect contacts. In studies of CD22-cytoskeleton interactions, we found that SPT was more sensitive to changes in cluster size than confocal microscopy. Furthermore, we examined CD22-cytoskeleton interactions using a range of CytoD concentrations (2.5–10  $\mu\text{g}/\text{mL}$ ), while previous studies tested only a single concentration and found no effect (15). The interaction of CD22 with the cytoskeleton was complex, and our data indicated that with low concentrations of CytoD (2.5  $\mu\text{g}/\text{mL}$ ), CD22 was found in larger

clusters with reduced lateral mobility. These data cannot resolve whether CD22-cytoskeleton contacts are direct or indirect, but it is well known that this receptor is found in homotypic clusters (5) and has *cis*-binding interactions with sialoglycoproteins such as CD45 (6,15,45,82). Notably, CD45 is associated with the cytoskeleton through a spectrin-ankyrin complex that regulates its lateral mobility, providing a likely explanation for these findings (83–85).

As a Siglec that engages *cis*-ligands, CD22 organization could be expected to be influenced by mechanisms that regulate membrane sialoglycoproteins. Previous work has found changes to CD22 organization from altered sialyltransferase expression, CD45 expression, lectin activity of CD22, and altered glycosylation sites on CD22 (15,52,86,87). Knockout of ST6Gal I results in reduced CD22 cluster size (88,89). Sialic acids may mask binding sites for galectins, which could regulate CD22 clustering and heterotypic interactions (87). This work is the first to explore the role of native NEU enzymes in CD22 organization. We found

that NEU1 and NEU3 had a role in CD22 clustering, and our data suggest that isoenzymes could play disparate roles in B cell regulation. There is growing recognition that native NEU enzymes may play important roles in inflammation and immune cells (22,30,90–92). We hypothesize that our observations of CD22 clustering and lateral mobility can be understood through a model that combines the influence of cytoskeletal interactions and interactions of CD22 receptor with its *cis*-ligands (Fig. 9). If we consider interactions between the cytoskeleton and CD45 (or other sialylated ligands) with CD22, the cluster size will be determined by the stoichiometry of these species (Fig. 9 A). Cytoskeletal contacts may help organize CD22 via indirect interactions with bridging glycoprotein ligands for CD22 (Figs. 9 A and C). This model accounts for our observation of increased CD22 clusters at low concentrations of cytoskeletal disruptors, which is reversed at higher concentrations. Furthermore, NEU activity that reduces sialoside concentration on the membrane will drive complex formation. Our results with NEU1 are consistent with this interpretation, as decreased NEU1 activity resulted in increased cluster size. We note that this model is consistent with experiments where a large excess of multivalent CD22 ligands reverses cell activation (10). Our NEU3 results are less consistent with alteration of total sialosides; instead, we propose that NEU3 activity may disrupt microdomain organization resulting in increased diffusion either through interactions with membrane proteins such as caveolin or through changes in glycolipid concentrations (93). Our results may suggest that changes in sialylation of B cell glycoconjugates during differentiation *in vivo* could be influenced by NEU enzymes (67). Current models of BCR activation suggest that the cytoskeleton acts to segregate BCR microclusters and that depolymerization of the cytoskeleton increases B cell activation by increasing encounters with co-receptors (34,94). Our findings suggest that CD22 organization is affected by cytoskeletal restriction. We submit that further investigation of the role of native NEU enzymes in B cell regulation is needed.

A common strategy to perturb CD22-ligand interactions is to treat cells with exogenous NEU. Many examples have tested the effect of exogenous bacterial NEU enzymes on CD22 organization and activity (15,52). While these reagents may reveal aspects of CD22-ligand interactions, they may not report on the role of native NEU isoenzymes. The substrate preferences of bacterial enzymes and native NEU are different. Enzymes like NanI prefer glycoprotein substrates, while NEU3 prefers glycolipids (95,96). NEU1 is known to prefer glycoprotein substrates but may have a role in ganglioside degradation (20,97). Furthermore, hNEU enzymes can have subtle differences in substrate

specificity (98). Glycosphingolipids are a major component of membrane microdomains, and these membrane components may be modulated by NEU3 activity (99). Bacterially produced enzymes may also be contaminated with LPSS, which we observed could alter CD22 clustering. Thus, we suggest that results based on the use of bacterially produced enzymes be interpreted with caution, and we favor the use of small-molecule inhibitors or KD of NEU expression to avoid this complication.

## SUPPORTING MATERIAL

Supporting material can be found online at <https://doi.org/10.1016/j.bpr.2022.100064>.

## AUTHOR CONTRIBUTIONS

Conceived and designed experiments, C.W.C., H.-T.T.T., and C.L.; performed experiments and analyzed data, H.-T.T.T., R.C., and C.L.; wrote the manuscript, C.W.C. and H.-T.T.T.

## ACKNOWLEDGMENTS

The authors would like to thank Dr. Matthew Macauley for providing murine hybridoma cells expressing anti-CD22 antibodies. This work was supported by grants from the Natural Sciences and Engineering Research Council of Canada (NSERC RGPIN-2020-04371) and the Canadian Glycomics Network (GlycoNet). A version of this manuscript has been posted at <https://biorxiv.org/cgi/content/short/2021.04.29.441886v1>.

## DECLARATION OF INTERESTS

C.W.C. is a co-inventor of a patent describing NEU inhibitors used in this study.

## REFERENCES

1. Nitschke, L., R. Carsetti, ..., M. C. Lamers. 1997. CD22 is a negative regulator of B-cell receptor signalling. *Curr. Biol.* 7:133–143. [https://doi.org/10.1016/S0960-9822\(06\)00057-1](https://doi.org/10.1016/S0960-9822(06)00057-1).
2. Ereño-Orbea, J., T. Sicard, ..., J.-P. Julien. 2017. Molecular basis of human CD22 function and therapeutic targeting. *Nat. Commun.* 8:764. <https://doi.org/10.1038/s41467-017-00836-6>.
3. Doody, G. M., L. B. Justement, ..., D. T. Fearon. 1995. A role in B cell activation for CD22 and the protein tyrosine phosphatase SHP. *Science.* 269:242–244. <https://doi.org/10.1126/science.7618087>.
4. Razi, N., and A. Varki. 1998. Masking and unmasking of the sialic acid-binding lectin activity of CD22 (Siglec-2) on B lymphocytes. *Proc. Natl. Acad. Sci. USA.* 95:7469–7474. <https://doi.org/10.1073/pnas.95.13.7469>.
5. Han, S., B. E. Collins, ..., J. C. Paulson. 2005. Homomultimeric complexes of CD22 in B cells revealed by protein-glycan cross-linking. *Nat. Chem. Biol.* 1:93–97. <https://doi.org/10.1038/nchembio713>.
6. Sgroi, D., G. A. Koretzky, and I. Stamenkovic. 1995. Regulation of CD45 engagement by the B-cell receptor CD22. *Proc. Natl. Acad.*

- Sci. USA.* 92:4026–4030. <https://doi.org/10.1073/pnas.92.9.4026>.
7. Law, C. L., A. Aruffo, ..., E. A. Clark. 1995. Ig domains 1 and 2 of murine CD22 constitute the ligand-binding domain and bind multiple sialylated ligands expressed on B and T cells. *J. Immunol.* 155:3368–3376.
  8. Nitschke, L. 2009. CD22 and Siglec-G: B-cell inhibitory receptors with distinct functions. *Immunol. Rev.* 230:128–143. <https://doi.org/10.1111/j.1600-065X.2009.00801.x>.
  9. Collins, B. E., O. Blixt, ..., J. C. Paulson. 2006. High-affinity ligand probes of CD22 overcome the threshold set by cis ligands to allow for binding, endocytosis, and killing of B Cells. *J. Immunol.* 177:2994–3003. <https://doi.org/10.4049/jimmunol.177.5.2994>.
  10. Courtney, A. H., E. B. Puffer, ..., L. L. Kiessling. 2009. Sialylated multivalent antigens engage CD22 *in trans* and inhibit B cell activation. *Proc. Natl. Acad. Sci. USA.* 106:2500–2505. <https://doi.org/10.1073/pnas.0807207106>.
  11. Macauley, M. S., F. Pfrengle, ..., J. C. Paulson. 2013. Antigenic liposomes displaying CD22 ligands induce antigen-specific B cell apoptosis. *J. Clin. Invest.* 123:3074–3083. <https://doi.org/10.1172/JCI69187>.
  12. Chen, W. C., G. C. Completo, ..., J. C. Paulson. 2010. In vivo targeting of B-cell lymphoma with glycan ligands of CD22. *Blood.* 115:4778–4786. <https://doi.org/10.1182/blood-2009-12-257386>.
  13. Duong, B. H. H. Tian, ..., D. Nemazee. 2010. Decoration of T-independent antigen with ligands for CD22 and Siglec-G can suppress immunity and induce B cell tolerance in vivo. *J. Exp. Med.* 207:173–187. <https://doi.org/10.1084/jem.20091873>.
  14. Daskhan, G. C., H.-T. T. Tran, ..., C. W. Cairo. 2018. Construction of Multivalent Homo- and Heterofunctional ABO Blood Group Glycoconjugates Using a Trifunctional Linker Strategy. *Bioconjug. Chem.* 29:343–362. <https://doi.org/10.1021/acs.bioconjchem.7b00679>.
  15. Gasparrini, F., C. Feest, ..., F. D. Batista. 2016. Nanoscale organization and dynamics of the siglec CD 22 cooperate with the cytoskeleton in restraining BCR signalling. *EMBO J.* 35:258–280. <https://doi.org/10.15252/embj.201593027>.
  16. He, X., T. A. Woodford-Thomas, ..., M. L. Thomas. 2002. Targeting of CD45 protein tyrosine phosphatase activity to lipid microdomains on the T cell surface inhibits TCR signaling. *Eur. J. Immunol.* 32:2578–2587. [https://doi.org/10.1002/1521-4141\(200209\)32:9<2578::AID-IMMU2578>3.0.CO;2-3](https://doi.org/10.1002/1521-4141(200209)32:9<2578::AID-IMMU2578>3.0.CO;2-3).
  17. Edmonds, S. D., and H. L. Ostergaard. 2002. Dynamic association of CD45 with detergent-insoluble microdomains in T lymphocytes. *J. Immunol.* 169:5036–5042. <https://doi.org/10.4049/jimmunol.169.9.5036>.
  18. Guo, B., R. M. Kato, ..., D. J. Rawlings. 2000. Engagement of the human Pre-B cell receptor generates a lipid raft-dependent calcium signaling complex. *Immunity.* 13:243–253. [https://doi.org/10.1016/S1074-7613\(00\)00024-8](https://doi.org/10.1016/S1074-7613(00)00024-8).
  19. Gupta, N., and A. L. DeFranco. 2003. Visualizing lipid raft dynamics and early signaling events during antigen receptor-mediated B-lymphocyte activation. *Mol. Biol. Cell.* 14:432–444. <https://doi.org/10.1091/mbc.02-05-0078>.
  20. Miyagi, T., and K. Yamaguchi. 2012. Mammalian sialidases: physiological and pathological roles in cellular functions. *Glycobiology.* 22:880–896.
  21. Glanz, V. Y., V. A. Myasoedova, ..., A. N. Orekhov. 2019. Sialidase activity in human pathologies. *Eur. J. Pharmacol.* 842:345–350. <https://doi.org/10.1016/j.ejphar.2018.11.014>.
  22. Demina, E. P., V. Smutova, ..., A. V. Pshezhetsky. 2021. Neuraminidases 1 and 3 trigger atherosclerosis by desialylating low-density lipoproteins and increasing their uptake by macrophages. *J. Am. Heart Assoc.* 10:e018756. <https://doi.org/10.1161/JAHA.120.018756>.
  23. Kato, T., Y. Wang, ..., T. Miyagi. 2001. Overexpression of lysosomal-type sialidase leads to suppression of metastasis associated with reversion of malignant phenotype in murine B16 melanoma cells. *Int. J. Cancer.* 92:797–804. <https://doi.org/10.1002/ijc.1268>.
  24. Sawada, M., S. Moriya, ..., T. Miyagi. 2002. Reduced sialidase expression in highly metastatic variants of mouse colon adenocarcinoma 26 and retardation of their metastatic ability by sialidase overexpression. *Int. J. Cancer.* 97:180–185. <https://doi.org/10.1002/ijc.1598>.
  25. Silvestri, I., F. Testa, ..., C. Tringali. 2014. Sialidase NEU4 is involved in glioblastoma stem cell survival. *Cell Death Dis.* 5:e1381. <https://doi.org/10.1038/cddis.2014.349>.
  26. Seyrantepe, V., S. A. Demir, ..., T. Miyagi. 2018. Murine Sialidase Neu3 facilitates GM2 degradation and bypass in mouse model of Tay-Sachs disease. *Exp. Neurol.* 299:26–41. <https://doi.org/10.1016/j.expneurol.2017.09.012>.
  27. Seyrantepe, V., K. Landry, ..., A. V. Pshezhetsky. 2004. Neu4, a novel human lysosomal lumen sialidase, confers normal phenotype to sialidosis and galactosialidosis cells. *J. Biol. Chem.* 279:37021–37029. <https://doi.org/10.1074/jbc.M404531200>.
  28. Hasegawa, T., N. Sugeno, ..., Y. Itoyama. 2007. Role of Neu4L sialidase and its substrate ganglioside GD3 in neuronal apoptosis induced by catechol metabolites. *FEBS Lett.* 581:406–412. <https://doi.org/10.1016/j.febslet.2006.12.046>.
  29. Igdoura, S. A., C. Mertineit, ..., R. A. Gravel. 1999. Sialidase-mediated depletion of GM2 ganglioside in Tay-Sachs neuroglia cells. *Hum. Mol. Genet.* 8:1111–1116. <https://doi.org/10.1093/hmg/8.6.1111>.
  30. Howlader, M. A., C. Li, ..., C. W. Cairo. 2019. Neuraminidase-3 is a negative regulator of LFA-1 adhesion. *Front. Chem.* 7:791. <https://doi.org/10.3389/fchem.2019.00791>.
  31. Wendt, E. R., H. Ferry, ..., S. Keshav. 2015. Ratiometric analysis of Fura Red by flow cytometry: a technique for monitoring intracellular calcium flux in primary cell subsets. *PLoS One.* 10:e0119532. <https://doi.org/10.1371/journal.pone.0119532>.
  32. Tolar, P., J. Hanna, ..., S. K. Pierce. 2009. The constant region of the membrane immunoglobulin mediates B cell-receptor clustering and signaling in response to membrane antigens. *Immunity.* 30:44–55. <https://doi.org/10.1016/j.immuni.2008.11.007>.
  33. Harwood, N. E., and F. D. Batista. 2011. The cytoskeleton coordinates the early events of B-cell activation. *Cold Spring Harb. Perspect. Biol.* 3:a002360. <https://doi.org/10.1101/cshperspect.a002360>.
  34. Treanor, B., D. Depoil, ..., F. D. Batista. 2010. The membrane skeleton controls diffusion dynamics and signaling through the B cell receptor. *Immunity.* 32:187–199. <https://doi.org/10.1016/j.immuni.2009.12.005>.
  35. Schliwa, M. 1982. Action of cytochalasin D on cytoskeletal networks. *J. Cell Biol.* 92:79–91. <https://doi.org/10.1083/jcb.92.1.79>.
  36. Goddette, D. W., and C. Frieden. 1986. The actin polymerization. The mechanism of action of Cytochalasin D. *J. Biol. Chem.* 261:15974–15980.
  37. Morton, W. M., K. R. Ayscough, and P. J. McLaughlin. 2000. Latrunculin alters the actin-monomer subunit interface to prevent polymerization. *Nat. Cell Biol.* 2:376–378. <https://doi.org/10.1038/35014075>.
  38. Coué, M., S. L. Brenner, ..., E. D. Korn. 1987. Inhibition of actin polymerization by latrunculin A. *FEBS Lett.* 213:316–318. [https://doi.org/10.1016/0014-5793\(87\)81513-2](https://doi.org/10.1016/0014-5793(87)81513-2).
  39. Wakatsuki, T., B. Schwab, ..., E. L. Elson. 2001. Actin polymerization and cell mechanics. *J. Cell Sci.* 114:1025–1036.
  40. Stevenson, B. R., and D. A. Begg. 1994. Concentration-dependent effects of cytochalasin D on tight junctions and actin filaments in MDCK epithelial cells. *J. Cell Sci.* 107:367–375.

41. Cai, S., X. Liu, ..., P. L. Kaufman. 2000. Effect of latrunculin-A on morphology and actin-associated adhesions of cultured human trabecular meshwork cells. *Mol. Vis.* 6:132–143.
42. Foissner, I., and G. O. Wasteneys. 2007. Wide-ranging effects of eight cytochalasins and latrunculin A and B on intracellular motility and actin filament reorganization in characean internodal cells. *Plant Cell Physiol.* 48:585–597. <https://doi.org/10.1093/pcp/pcm030>.
43. Jaqaman, K., D. Loerke, ..., G. Danuser. 2008. Robust single-particle tracking in live-cell time-lapse sequences. *Nat. Methods.* 5:695–702. <https://doi.org/10.1038/nmeth.1237>.
44. Ramya, T. N. C., E. Weerapana, ..., J. C. Paulson. 2010. In situ trans ligands of CD22 identified by glycan-protein photocross-linking-enabled proteomics. *Mol. Cell. Proteomics.* 9:1339–1351. <https://doi.org/10.1074/mcp.m900461-mcp200>.
45. Zhang, M., and A. Varki. 2004. Cell surface sialic acids do not affect primary CD22 interactions with CD45 and surface IgM nor the rate of constitutive CD22 endocytosis. *Glycobiology.* 14:939–949. <https://doi.org/10.1093/glycob/cwh126>.
46. Coughlin, S., M. Noviski, ..., J. Zikherman. 2015. An extracatalytic function of CD45 in B cells is mediated by CD22. *Proc. Natl. Acad. Sci. USA.* 112:E6515–E6524. <https://doi.org/10.1073/pnas.1519925112>.
47. Alborzian Deh Sheikh, A., C. Akatsu, ..., T. Tsubata. 2018. Proximity labeling of cis-ligands of CD22/Siglec-2 reveals stepwise  $\alpha$ 2, 6 sialic acid-dependent and -independent interactions. *Biochem. Biophys. Res. Commun.* 495:854–859. <https://doi.org/10.1016/j.bbrc.2017.11.086>.
48. Heiser, W. C. 2000. Optimizing electroporation conditions for the transformation of mammalian cells. In *Transcription Factor Protocols*. M. J. Tymms, ed. Humana Press, pp. 117–134. <https://doi.org/10.1385/1-59259-686-X:117>.
49. Sandbhor, M. S., N. Soya, ..., C. W. Cairo. 2011. Substrate recognition of the membrane-associated sialidase NEU3 requires a hydrophobic aglycone. *Biochemistry.* 50:6753–6762.
50. Kaminuma, O., S. Katoh, ..., T. Hiroi. 2018. Contribution of neuraminidase 3 to the differentiation of induced regulatory T cells. *Gene Cell.* 23:112–116. <https://doi.org/10.1111/gtc.12553>.
51. Nan, X., I. Carubelli, and N. M. Stamatou. 2007. Sialidase expression in activated human T lymphocytes influences production of IFN- $\gamma$ . *J. Leukoc. Biol.* 81:284–296. <https://doi.org/10.1189/jlb.1105692>.
52. Meyer, S. J., A. T. Linder, ..., L. Nitschke. 2018. B cell siglecs—news on signaling and its interplay with ligand binding. *Front. Immunol.* 9:2820. <https://doi.org/10.3389/fimmu.2018.02820>.
53. Gryniewicz, G., M. Poenie, and R. Y. Tsien. 1985. A new generation of Ca<sup>2+</sup> indicators with greatly improved fluorescence properties. *J. Biol. Chem.* 260:3440–3450. [https://doi.org/10.1016/S0021-9258\(19\)83641-4](https://doi.org/10.1016/S0021-9258(19)83641-4).
54. Schepers, E., G. Glorieux, ..., R. Vanholder. 2009. Flow cytometric calcium flux assay: Evaluation of cytoplasmic calcium kinetics in whole blood leukocytes. *J. Immunol. Methods.* 348:74–82. <https://doi.org/10.1016/j.jim.2009.07.002>.
55. Cairo, C. W. 2014. Inhibitors of the human neuraminidase enzymes. *MedChemComm.* 5:1067–1074. <https://doi.org/10.1039/C4MD00089G>.
56. Richards, M. R., T. Guo, ..., C. W. Cairo. 2018. Molecular dynamics simulations of viral neuraminidase inhibitors with the human neuraminidase enzymes: Insights into isoenzyme selectivity. *Bioorg. Med. Chem.* 26:5349–5358. <https://doi.org/10.1016/j.bmc.2018.05.035>.
57. Guo, T., P. Dätwyler, ..., C. W. Cairo. 2018. Selective inhibitors of human neuraminidase 3. *J. Med. Chem.* 61:1990–2008. <https://doi.org/10.1021/acs.jmedchem.7b01574>.
58. Guo, T., R. Héon-Roberts, ..., C. W. Cairo. 2018. Selective inhibitors of human neuraminidase 1 (NEU1). *J. Med. Chem.* 61:11261–11279. <https://doi.org/10.1021/acs.jmedchem.8b01411>.
59. Uchida, Y., Y. Tsukada, and T. Sugimori. 1979. Enzymatic properties of neuraminidases from *Arthrobacter urefae*ns. *J. Biochem.* 86:1573–1585. <https://doi.org/10.1093/oxfordjournals.jbchem.a132675>.
60. Ohta, Y., Y. Tsukada, and T. Sugimori. 1989. Purification and properties of neuraminidase isozymes in *Arthrobacter urefae*ns mutant. *J. Biochem.* 106:1086–1089. <https://doi.org/10.1093/oxfordjournals.jbchem.a122969>.
61. Wang, Y. H. 2020. Sialidases from *Clostridium perfringens* and their inhibitors. *Front. Cell. Infect. Microbiol.* 9:11. <https://doi.org/10.3389/fcimb.2019.00462>.
62. Sato, S., A. S. Miller, ..., T. F. Tedder. 1996. CD22 is both a positive and negative regulator of B lymphocyte antigen receptor signal transduction: altered signaling in CD22-deficient mice. *Immunity.* 5:551–562. [https://doi.org/10.1016/S1074-7613\(00\)80270-8](https://doi.org/10.1016/S1074-7613(00)80270-8).
63. Rahman, H., M. Qasim, ..., A. R. Asif. 2011. Fetal calf serum heat inactivation and lipopolysaccharide contamination influence the human T lymphoblast proteome and phosphoproteome. *Proteome Sci.* 9:71. <https://doi.org/10.1186/1477-5956-9-71>.
64. Koenig, S., and M. K. Hoffmann. 1979. Bacterial lipopolysaccharide activates suppressor B lymphocytes. *Proc. Natl. Acad. Sci. USA.* 76:4608–4612. <https://doi.org/10.1073/pnas.76.9.4608>.
65. Lajaunias, F., L. Nitschke, ..., S. Izui. 2002. Differentially regulated expression and function of CD22 in activated B-1 and B-2 lymphocytes. *J. Immunol.* 168:6078–6083. <https://doi.org/10.4049/jimmunol.168.12.6078>.
66. Carnahan, J., P. Wang, ..., J. Sun. 2009. Epratuzumab, a humanized monoclonal antibody targeting CD22: characterization of in vitro properties. *Clin. Cancer Res.* 9:3982s–3990s.
67. Giovannone, N., A. Antonopoulos, ..., C. J. Dimitroff. 2018. Human B cell differentiation is characterized by progressive remodeling of O-linked glycans. *Front. Immunol.* 9:2857. <https://www.frontiersin.org/article/10.3389/fimmu.2018.02857>.
68. Giovannone, N., J. Liang, ..., C. J. Dimitroff. 2018. Galectin-9 suppresses B cell receptor signaling and is regulated by I-branching of N-glycans. *Nat. Commun.* 9:3287. <https://doi.org/10.1038/s41467-018-05770-9>.
69. Tanaka, K. A. K., K. G. N. Suzuki, ..., A. Kusumi. 2010. Membrane molecules mobile even after chemical fixation. *Nat. Methods.* 7:865–866. <https://doi.org/10.1038/nmeth.f.314>.
70. Cairo, C. W., and D. E. Golan. 2008. T cell adhesion mechanisms revealed by receptor lateral mobility. *Biopolymers.* 89:409–419.
71. Ramadurai, S., A. Holt, ..., B. Poolman. 2009. Lateral diffusion of membrane proteins. *J. Am. Chem. Soc.* 131:12650–12656. <https://doi.org/10.1021/ja902853g>.
72. Auth, T., and N. S. Gov. 2009. Diffusion in a fluid membrane with a flexible cortical cytoskeleton. *Biophys. J.* 96:818–830. <https://doi.org/10.1016/j.bpj.2008.10.038>.
73. Saha, S., I.-H. Lee, ..., S. Mayor. 2015. Diffusion of GPI-anchored proteins is influenced by the activity of dynamic cortical actin. *Mol. Biol. Cell.* 26:4033–4045. <https://doi.org/10.1091/mbc.E15-06-0397>.
74. Gómez-Llobregat, J., J. Buceta, and R. Reigada. 2013. Interplay of cytoskeletal activity and lipid phase stability in dynamic protein recruitment and clustering. *Sci. Rep.* 3:2608. <https://doi.org/10.1038/srep02608>.
75. Koppel, D. E., M. P. Sheetz, and M. Schindler. 1981. Matrix control of protein diffusion in biological membranes. *Proc. Natl. Acad. Sci. USA.* 78:3576–3580. <https://doi.org/10.1073/pnas.78.6.3576>.
76. Lenne, P.-F., L. Wawrezynieck, ..., D. Marguet. 2006. Dynamic molecular confinement in the plasma membrane by microdomains and the cytoskeleton meshwork. *EMBO J.* 25:3245–3256. <https://doi.org/10.1038/sj.emboj.7601214>.
77. Javanainen, M., H. Martinez-Seara, ..., I. Vattulainen. 2017. Diffusion of integral membrane proteins in protein-rich membranes.

- J. Phys. Chem. Lett.* 8:4308–4313. <https://doi.org/10.1021/acs.jpcclett.7b01758>.
78. Zhang, M., M. Moran, ..., M. C. Miceli. 2005. CD45 signals outside of lipid rafts to promote ERK activation, synaptic raft clustering, and IL-2 production. *J. Immunol.* 174:1479–1490. <https://doi.org/10.4049/jimmunol.174.3.1479>.
  79. Mielenz, D., C. Vettermann, ..., H. M. Jäck. 2005. Lipid rafts associate with intracellular B cell receptors and exhibit a B cell stage-specific protein composition. *J. Immunol.* 174:3508–3517. <https://doi.org/10.4049/jimmunol.174.6.3508>.
  80. Gupta, N., B. Wollscheid, ..., A. L. DeFranco. 2006. Quantitative proteomic analysis of B cell lipid rafts reveals that ezrin regulates antigen receptor-mediated lipid raft dynamics. *Nat. Immunol.* 7:625–633. <https://doi.org/10.1038/ni1337>.
  81. Kabouridis, P. S., and E. C. Jury. 2008. Lipid rafts and T-lymphocyte function: Implications for autoimmunity. *FEBS Lett.* 582:3711–3718. <https://doi.org/10.1016/j.febslet.2008.10.006>.
  82. Bakker, T. R., C. Piperi, and E. A. Davies. 2002. Comparison of CD22 binding to native CD45 and synthetic oligosaccharide. *Eur. J. Immunol.* 32:1924–1932. [https://doi.org/10.1002/1521-4141\(200207\)32:7<1924::AID-IMMU1924>3.0.CO;2-N](https://doi.org/10.1002/1521-4141(200207)32:7<1924::AID-IMMU1924>3.0.CO;2-N).
  83. Cairo, C. W., R. Das, ..., D. E. Golan. 2010. Dynamic regulation of CD45 lateral mobility by the Spectrin-Ankyrin cytoskeleton of T cells. *J. Biol. Chem.* 285:11392–11401. <https://doi.org/10.1074/jbc.M109.075648>.
  84. Pradhan, D., and J. Morrow. 2002. The Spectrin-Ankyrin skeleton controls CD45 surface display and interleukin-2 production. *Immunity.* 17:303–315. [https://doi.org/10.1016/S1074-7613\(02\)00396-5](https://doi.org/10.1016/S1074-7613(02)00396-5).
  85. Lokeshwar, V. B., and L. Y. Bourguignon. 1992. Tyrosine phosphatase activity of lymphoma CD45 (GP180) is regulated by a direct interaction with the cytoskeleton. *J. Biol. Chem.* 267:21551–21557. [https://doi.org/10.1016/S0021-9258\(19\)36645-1](https://doi.org/10.1016/S0021-9258(19)36645-1).
  86. Collins, B. E., O. Blixt, ..., J. C. Paulson. 2002. Constitutively unmasked CD22 on B cells of ST6Gal I knockout mice: novel sialoside probe for murine CD22. *Glycobiology.* 12:563–571. <https://doi.org/10.1093/glycob/cwf067>.
  87. Wasim, L., F. H. M. Buhari, ..., B. Treanor. 2019. N-linked glycosylation regulates CD22 organization and function. *Front. Immunol.* 10:699. <https://doi.org/10.3389/fimmu.2019.00699>.
  88. Collins, B. E., B. A. Smith, ..., J. C. Paulson. 2006. Ablation of CD22 in ligand-deficient mice restores B cell receptor signaling. *Nat. Immunol.* 7:199–206. <https://doi.org/10.1038/ni1283>.
  89. Grewal, P. K., M. Botton, ..., J. D. Marth. 2006. ST6Gal-I restrains CD22-dependent antigen receptor endocytosis and Shp-1 recruitment in normal and pathogenic immune signaling. *Mol. Cell Biol.* 26:4970–4981. <https://doi.org/10.1128/MCB.00308-06>.
  90. Gadhroum, S. Z., and R. Sackstein. 2008. CD15 expression in human myeloid cell differentiation is regulated by sialidase activity. *Nat. Chem. Biol.* 4:751–757. <https://doi.org/10.1038/nchembio.116>.
  91. Luzina, I. G., E. P. Lillehoj, ..., S. E. Goldblum. 2021. Therapeutic effect of neuraminidase-1-selective inhibition in mouse models of bleomycin-induced pulmonary inflammation and fibrosis. *J. Pharmacol. Exp. Ther.* 376:136–146. <https://doi.org/10.1124/jpet.120.000223>.
  92. Howlader, M. A., E. P. Demina, ..., C. W. Cairo. 2022. The Janus-like role of neuraminidase isoenzymes in inflammation. *FASEB J.* 36:e22285. <https://doi.org/10.1096/fj.202101218R>.
  93. Bonardi, D., N. Papini, ..., R. Bresciani. 2014. Sialidase NEU3 dynamically associates to different membrane domains specifically modifying their ganglioside pattern and triggering Akt phosphorylation. *PLoS One.* 9:e99405. <https://doi.org/10.1371/journal.pone.0099405>.
  94. Mattila, P. K., F. D. Batista, and B. Treanor. 2016. Dynamics of the actin cytoskeleton mediates receptor cross talk: An emerging concept in tuning receptor signaling. *J. Cell Biol.* 212:267–280. <https://doi.org/10.1083/jcb.201504137>.
  95. Roggentin, P., R. G. Kleineidam, and R. Schauer. 1995. Diversity in the properties of two sialidase isoenzymes produced by *Clostridium perfringens* spp. *Biol. Chem. Hoppe Seyler.* 376:569–575.
  96. Wang, Y., K. Yamaguchi, ..., T. Miyagi. 2001. Site-directed mutagenesis of human membrane-associated ganglioside sialidase - identification of amino-acid residues contributing to substrate specificity. *Eur. J. Biochem.* 268:2201–2208.
  97. Timur, Z. K., S. Akyildiz Demir, ..., V. Seyrantepe. 2015. Neuraminidase-1 contributes significantly to the degradation of neuronal B-series gangliosides but not to the bypass of the catabolic block in Tay–Sachs mouse models. *Mol. Genet. Metab. Rep.* 4:72–82. <https://doi.org/10.1016/j.ymgmr.2015.07.004>.
  98. Smutova, V., A. Albohy, ..., A. V. Pshezhetsky. 2014. Structural Basis for Substrate Specificity of Mammalian Neuraminidases. *PLoS One.* 9:e106320. <https://doi.org/10.1371/journal.pone.0106320>.
  99. Simons, K., and D. Toomre. 2000. Lipid rafts and signal transduction. *Nat. Rev. Mol. Cell Biol.* 1:31–39. <https://doi.org/10.1038/35036052>.